Title: Tree growth sensitivity to climate varies across a seasonal precipitation gradient

Larissa L. Yocom[1,*], Kiona Ogle[2,3], Drew Peltier[3], Paul Szejner[4,5], Yao Liu[6,7], Russell K. Monson[5,8]

[1]Department of Wildland Resources and the Ecology Center, Utah State University, 5230 Old Main, Logan, UT, USA

[2]School of Informatics, Computing, and Cyber Systems, Northern Arizona University, Flagstaff, AZ

[3]Department of Biological Sciences, Northern Arizona University, Flagstaff, AZ

[4]Instituto de Geología, Universidad Nacional Autónoma de México, México City, México

[5]Laboratory of Tree-Ring Research, University of Arizona, Tucson, AZ[1]

[6]Environmental Sciences Division and Climate Change Science Institute, Oak Ridge National Laboratory, Oak Ridge, TN, USA*

[7]Current affiliation: Department of Geography and Environmental Sciences, Northumbria University, Newcastle upon Tyne, UK

[8]Department of Ecology and Evolutionary Biology, University of Arizona, Tucson, AZ

*Correspondence author, larissa.yocom@usu.edu, 435-797-4155

LLY and KO conceived of the idea. PS and RKM collected the data. LLY, KO and DP analyzed the data. LLY wrote the manuscript; all authors provided editorial advice.

Abstract:

Spatial patterns of precipitation in the southwestern United States result in a complex gradient from winter to summer moisture dominance that influences tree growth. In response, tree growth exhibits seasonal-to-annual variability that is evident in the growth of whole tree rings, or sub-annual sections such as earlywood and latewood. We evaluated the influence of precipitation and temperature on the growth of *Pinus ponderosa* trees in 11 sites in the southwestern US. Precipitation during the year of growth and the prior year accounted for about half of the climate influence on annual growth, with the other half reflecting conditions 2-4 years prior to growth, indicating that individual trees do indeed exhibit multi-year "memory" of climate. Trees in wetter sites exhibited weaker influence of past precipitation inputs, but longer memory of climatic variability. Conversely, trees in dry sites exhibited shorter memory of long-term climatic variability, but greater sensitivity to past precipitation effects. These results are consistent with the existence of complex interactions between endogenous (phenotype) effects and exogenous (climate) effects in controlling climate memory in trees. After accounting for climate, residual variability in latewood growth was negatively correlated with earlywood growth, indicating a potential trade-off between latewood versus earlywood growth. This study provides new insights that will assist the accurate prediction of woody biomass growth and forest carbon sequestration across a southwestern US precipitation gradient.

Key words: Bayesian, dendrochronology, memory, monsoon, *Pinus ponderosa*

Introduction

Annual tree-ring growth integrates the interactions of numerous physiological processes with climate variability at subannual to multi-year time scales (Fritts 1976, Salzer and Kipfmueller 2005, Stahle et al. 2009, Griffin et al. 2013, Peltier et al. 2016, 2018). The responsiveness of tree-ring widths to climate during the year of ring formation, and often during the prior year, has enabled their use in reconstructing past patterns of climate variables, such as precipitation and temperature (e.g., Salzer et al. 2005, Stahle et al. 2009, Griffin et al. 2011, 2013, Esper et al. 2018). However, annual ring widths are also influenced by climate over multiple years, whereby climate signals from several seasons prior to ring formation are detectable (Ogle et al. 2015, Peltier et al. 2016, 2018, Marqués et al. 2021).

Within individual annual rings in trees from temperate ecosystems, particularly conifers, there is variation in wood cell structure that reflects seasonal climate variations. Light-colored earlywood consists of large, thin-walled cells formed early in the growing season. Darker-colored latewood is formed later in the growing season and is characterized by smaller lumen area with thicker cell walls. Sub-annual patterns of earlywood and latewood can be used to inform intra-annual climate-growth relationships, particularly in regions with strong seasonal climatic patterns (Griffin et al. 2013, Babst et al. 2016, Monson et al. 2018, Szejner et al. 2016). Earlywood growth can be related to temperature (e.g., Zhang et al. 2021) but is often correlated with the amount of winter and spring precipitation received (for example, November through May; [Stahle et al. 2009]). Latewood width has been found to record a summer precipitation signal, especially if its dependence on earlywood growth is statistically removed (Stahle et al. 2009, Griffin et al. 2013, Szejner et al. 2018). It has been thought that earlywood and latewood are dependent on different sources of water because ring widths and seasonally-recorded oxygen

isotopes in the two types of wood have been found to correlate with precipitation in different seasons: winter precipitation for earlywood, and summer rainfall for latewood (Belmecheri et al. 2018, Ziaco et al. 2018, Szejner et al. 2018). However, there has been little research on the extent to which the growth of earlywood and latewood in the current year integrates climate over multiple prior years, or potential carbon allocation trade-offs between tree investment in earlywood versus latewood growth once climate-specific effects have been reconciled.

Summer rains in the southwestern United States (hereafter, "Southwest") are delivered by the North American Monsoon (NAM) climate system (Fig. 1). The NAM is characterized by frequent convective rain events that generally begin in early July in the Southwest and continue through September, following very dry conditions in May and June (Adams and Comrie 1997, Higgins et al. 1997). There is high variability in NAM precipitation at seasonal, annual, and decadal timescales (Higgins et al. 2003, Adams et al. 2014), and in the annual timing of NAM onset (Higgins et al. 1999). Geographically, there is a northwest-to-southeast gradient from winter-to-summer moisture dominance in the Southwest, with summer rainfall dominant in the southeast and winter precipitation dominant in the northwest (Fig. 1a). At the extreme of the gradient, >70% of annual rainfall is contributed by the NAM in parts of southern Arizona and New Mexico (Douglas et al. 1993, Szejner et al. 2016). Thus, depending on location, the NAM provides a significant moisture resource that potentially influences the growth, structure, and community composition of vegetation in the Southwest (Neilson 1987).

However, there are other patterns in precipitation across the region as well. There is a gradient in total annual precipitation from east-to-west, with greater precipitation in eastern New Mexico, grading to less precipitation in western Arizona. Within these regional patterns, precipitation increases with elevation (Fig. 1b). Variability of annual precipitation amount is

67 highly correlated with total annual precipitation amount – i.e., there is generally a higher
68 standard deviation in precipitation among years in areas with higher mean annual precipitation
69 (Fig. 1c). Because of the strong gradients in summer and annual precipitation across the region
70 and the variability in precipitation inherent in the regional climate system, the Southwest
71 represents an excellent location to test the influence of seasonal precipitation as well as its
72 variability on tree growth, including in the sub-annual components of tree rings.
73 The stochastic antecedent modeling (SAM) framework was developed to evaluate
74 antecedent factors (e.g., climate drivers) and their influence on physiological processes such as
75 tree growth (Ogle et al. 2015, Peltier et al. 2018). The SAM framework provides a quantitative
76 method of analyzing the importance of "ecological memory"—that is, the influence of
77 antecedent conditions on current processes (Ogle et al. 2015). An advantage of the SAM
78 approach is that the strength and temporal lags of each variable driving growth can be evaluated
79 simultaneously. Thus, we can reconstruct the roles of multiple exogenous and endogenous
80 processes in the ecophysiological memory of trees. In the current study, we applied this approach
81 to annual and intra-annual tree growth increments using *Pinus ponderosa* trees distributed across
82 a broad geographic precipitation gradient selected specifically to study variation in tree growth
83 processes across varied precipitation conditions. In doing so, we addressed three primary
84 questions: 1) Over what time scales (e.g., past monthly, seasonal, or annual periods) are climate
85 influences on tree growth evident? 2) Do tree growth sensitivity to climate and ecological
86 memory vary across the precipitation gradient? 3) Do earlywood and latewood growth differ in
87 their sensitivities to climate and climatic memory? Addressing these questions will provide
88 insight into the complexities of the responses of earlywood, latewood, and whole rings to
89 antecedent climate, helping us to disentangle the endogenous and exogenous mechanisms

underlying tree growth responses to variation in climate. Our study has implications for understanding drought impacts and forest functioning, in general, given current and future climatic variation, and within the more specific context of regional climate attributes.

Methods

Data description

To answer our questions, we used a set of tree cores previously collected for a related tree-ring isotope study (Szejner et al. 2016). Tree cores with at least five decades of growth were collected from ponderosa pine trees (*Pinus ponderosa* Dougl. ex Laws.) in 11 sites, with five sites in AZ, four in NM, and two in UT (Fig. 1; Szejner et al. 2016). Sites were located in ponderosa pine-dominated landscapes with low tree-to-tree canopy competition. Healthy, medium-sized trees were selected at each site (Szejner et al. 2016). Using a 5 mm increment borer, 2-3 cores were taken from each of 128 selected trees for a total of 266 cores (Table S1). In the laboratory, cores were crossdated using standard dendrochronology techniques (Stokes and Smiley 1968), and total ring, earlywood, and latewood widths of each ring were measured (Szejner et al. 2016).

Monthly precipitation and mean maximum monthly temperature data from 1895 to 2014 for each site were extracted from the PRISM gridded climate dataset (PRISM 2018) at the 30-m pixel resolution representing each site location. We considered using other climate indices (e.g., Palmer Drought Severity Index, vapor pressure deficit, minimum monthly temperature), but exploratory analyses of relationships between ring widths and these alternative indices led us to focus on simple precipitation and temperature variables. Precipitation and temperature, while not wholly representative of drought stress, are consistently and reliably measured and widely interpreted, and they include no built-in time-lags (such as those within PDSI).

Statistical model description

We used the stochastic antecedent modeling (SAM) approach developed by Ogle et al. (2015), which has been used in multiple applications (e.g., Liu et al. 2019, Guo et al. 2020), including several applications to estimate the effects that climatic variables have on tree growth as well as the time scales over which such variables influence growth (Peltier et al. 2018, 2019, 2021, Marqués et al. 2021). This model regresses ring widths (growth) on antecedent climate variables, while simultaneously estimating the time-scales over which the antecedent variables are defined, thus providing insight into lags and memory effects. That is, climatic variables affecting growth, as well as previous ring-width values, are used to construct antecedent variables, which themselves are defined as weighted averages of past observed values. The antecedent variables serve as covariates in the regression model, where each antecedent variable has its own effect parameter.

We assumed that observed, log-transformed ring widths, r = log(ring width + 1), for each core, c, and year, y, were normally distributed around the mean, $\mu_{y,c}$, with variance, σ^2:

$$r_{y,c} \sim Normal(\mu_{y,c}, \sigma^2) \quad (1)$$

Note that 1 was added to each ring width before log transforming to account for zero values due to missing rings (0.4% of rings were missing). We modeled μ as a function of ring age (A), antecedent precipitation (P^{ant}; see Eqn 5), antecedent maximum temperature (T^{ant}; see Eqn 5), the $P^{ant} \times T^{ant}$ two-way interaction, and log-scale prior ring width (rw^{ant}):

$$\mu_{y,c} = \varepsilon_c + \alpha_{t(c),2}\, A_{y,c} + \alpha_{t(c),3}\, P^{ant}_{y,s(c)} + \alpha_{t(c),4}\, T^{ant}_{y,s(c)} + \alpha_{t(c),5}\, P^{ant}_{y,s(c)} \times T^{ant}_{y,s(c)} + \alpha_{t(c),6}\, rw^{ant}_{y,c} \quad (2)$$

The nested notation $t(c)$ and $s(c)$ denote the tree, t, and site, s, corresponding to core c, respectively. Again, the model for μ in Eqn (2) is essentially a linear regression, conditional on the antecedent covariates and ring age (hence, detrending for age is accomplished simultaneously

within the model). Because μ represents log-transformed ring widths, the "linear age" effect on the log scale actually represents an exponential age function. The model includes a core-level intercept, or random effect (ε_c), that is modeled hierarchically around a tree-level intercept term, $\alpha_{t,1}$:

$$\varepsilon_c \sim Normal(\alpha_{t(c),1}, \sigma_\varepsilon^2) \quad (3)$$

See Table 1 for a summary of the parameters (coefficients) in Eqns (2) and (3).

To account for the field sampling scheme, where trees were sampled in 11 sites, we specified hierarchical priors for the tree-level α parameters, which varied around site-level means (a); site-level means were modeled as varying around a population- or species-level mean (a^*). Thus, for parameter $k = 1, 2, \ldots, 6$, tree t, and site s:

$$\begin{aligned} \alpha_{t,k} &\sim Normal(a_{s(t),k}, \sigma_{\alpha_k}^2) \\ a_{s,k} &\sim Normal(a_k^*, \sigma_{a_k}^2) \end{aligned} \quad (4)$$

Where $s(t)$ denotes site s associated with tree t. The variance terms σ_α^2 and σ_a^2 describe how parameter k varies among trees within each site and among sites, respectively. Finally, we assigned relatively non-informative priors to the population-level means and all standard deviation terms (σ in Eqn (1), σ_ε in Eqn (3), and σ_α and σ_a in Eqn (4)). That is, each a_k^* was assigned a wide, normally-distributed prior with mean 0 and standard deviation 10,000; each standard deviation term was assigned a wide, uniform prior between 0 and 100.

Defining the model covariates

The age of each tree t at the time of coring (i.e., the "final age") was not always known given that many cores did not include the pith. Thus, we treated the final age, A^{final}, of each tree as unknown, resulting in unknown age for each ring (A) such that:

$$A_{y,c} = A_{t(c)}^{final} - \delta_y \quad (5)$$

where δ_y is the number of rings produced after year y; e.g., if the most recent ring is 2012, then δ_y = 0, 1, 2, …, when y corresponds to 2012, 2011, 2010, …, respectively. Again, A^{final} is treated as an unknown quantity that is estimated for each tree (δ is known data). Thus, we assigned a vague (wide) uniform prior to each A_t^{final} with the lower limit set equal to the number of rings measured in tree t and the upper limit set to 1000.

We centered covariates to improve parameter interpretation and model convergence. Ring age, A, was centered about the estimated average ring age, $\bar{A}$ (~120 years), in all cores across all 11 sites; the antecedent climate variables were centered about the mean monthly values for each site ($\bar{P}$ and $\bar{T}$); and the antecedent ring widths, rw^{ant}, were centered about the average ring width recorded for each tree ($\overline{rw}$). Thus, the intercept (e.g., $\alpha_{t,1}$ in Eqn (3)) is the predicted, log-scale growth of tree t at an age of 120 years under average climatic and growth conditions (Table 1).

Furthermore, the antecedent variables (P^{ant}, T^{ant}, and rw^{ant}) are defined as weighted averages of past monthly (P^{ant} and T^{ant}) and yearly (rw^{ant}) values. For $X = P$ or T, the antecedent climate variables are defined as:

$$X_{y,s}^{ant} = \sum_{j=0}^{4} \sum_{m=1}^{12} \omega_{j,m,s,X} X_{y-j,m,s} \tag{6}$$

The antecedent importance weights, ω, are unknown and determined by fitting the model to the tree-ring and climate data. The importance weights can reveal time scales in the influences of past climate. Each climate variable at each site gets its own set of importance weights, as indicated by the s (site) and X subscripts on ω. The term $X_{y-j,m,s}$ is the precipitation total or maximum temperature for month m (m = 1, 2, …, 12 for Jan., Feb., …, Dec.), j years prior to the current year y, in site s. The weighted monthly climate values are summed over all months (m =

1, 2, …., 12), from $j = 0$ (year of ring formation) to $j = 4$ (4 years prior). The weights for current-year October through December ($m = 10, 11, 12$; $j = 0$) were set to 0 since we assumed the climate in these months occurred after growth ended and had no effect on current-year ring widths (McDowell et al. 2010). Monthly importance weights were estimated individually for the year of ring formation and one year prior ($j = 0$ and 1), but estimated in blocks of 2 months for two years prior to growth ($j = 2$) and in blocks of 3 months for three and four years prior to growth ($j = 3$ and 4; see Fig. 2 in Peltier et al. 2018). This results in a total of 35 importance weights, which were constrained to sum to 1 for each climate variable within each site; hence, each $\omega_{j,m,s,X}$ indicates the relative importance of climate variable X at site s in a particular time period (j and m).

Antecedent ring width, rw^{ant} in Eqn (2), was calculated similarly to the antecedent climate variables, but since ring widths are only reported at an annual scale, rw^{ant} is given by:

$$rw_{y,c}^{ant} = \sum_{j=1}^{4} w_{j,s} rw_{y-j,c} \quad (7)$$

The $rw_{y-j,c}$ term denotes the annual ring width (not log transformed) grown j years ($j = 1, 2, 3, 4$) prior to the current year's growth in year y. Here, $w_{j,s}$ denotes the relative importance of growth (ring width) j years prior to the current year at site s. Again, these antecedent weights were constrained to sum to 1 for each site s.

We assigned each group of antecedent importance weights—for precipitation, temperature, and past ring widths—a vague Dirichlet prior, *Dirichlet*(1,1,…,1), resulting in the prior expectation that all weights were the same (Ogle et al. 2015, Peltier et al. 2018). This prior also ensures that the weights sum to 1 and are each between 0 and 1.

Model implementation and further analyses

We implemented the above model, Eqns (1)-(7), separately for whole-ring, earlywood,

and latewood ring widths. The model structure was the same for the whole-ring and earlywood analyses, but it was modified for the latewood model by incorporating the earlywood ring width of the same year as a predictor in Eqn (2), with its corresponding effect parameter, $\alpha_{t(c),7}$ (e.g., Griffin et al. 2011), which was also assigned a hierarchical prior following Eqn (4). This was done so that we could estimate the conditional effect of earlywood growth given that climate, ring age, and past ring width effects are simultaneously accounted for. We centered earlywood ring widths about the average value reported for each tree *t*.

For the climate variables, we performed several calculations with the importance weights to provide greater insight into time-scales and influence and memory. For example, we computed annual importance weights by summing monthly importance weights, $\omega_{j,m,s,X}$ in Eqn (6), over all months *m* within each year *j*. For each climate variable, we also determined the number of months it took for each site to reach 50% of its cumulative monthly importance weight, which we refer to as M_{50}, following the definition in Ogle et al. (2015). M_{50} provides an index of the length of the climate memory (Ogle et al. 2015). Since months 10-12 (Oct-Dec) of the current year are assigned importance weight values of zero, this restricts M_{50} to be greater than 3 months. These quantities are computed within the model code (see below), enabling posterior estimates of each.

Using a high-performance computing cluster, we ran the model via the Bayesian software JAGS 4.2.0 (Plummer 2003) in R (R Core Team 2018) with the packages 'rjags' (Plummer 2013) and 'coda' (Plummer et al. 2006). Following standard practice to use multiple chains, we assigned different initial values to three parallel Markov chain Monte Carlo (MCMC) sequences and ran the sequences until they converged (>100,000 iterations). After convergence, we used a posterior sample size of ≥3000 relatively independent posterior samples after thinning to obtain

parameter estimates, including the posterior mean, standard deviation, and 95% credible interval (CI), defined by the 2.5th and 97.5th percentiles of the posterior samples.

Post-analysis growth responses across climatic gradients

We used the posterior parameter estimates to explore relationships between parameters describing the sensitivity of growth to climate (i.e., the site-level $a_{s,3}$, $a_{s,4}$, and $a_{s,5}$ effects; Table 1) and factors related to the variability in precipitation across the Southwest such as average precipitation, % of precipitation that falls in the summer, and annual, summer, and winter precipitation variability. For seasonal climate variables, we defined winter as December through March, and summer as July through September (Higgins et al. 1997). We performed a simple model comparison among these post-hoc models with single variables, which were linear regressions of the site-specific posterior parameter means versus site-level covariates.

Results

Model fit

A regression of observed versus mean predicted values of r = log(ring width + 1) resulted in coefficients of determination (R^2) of 0.86, 0.84, and 0.74 for the whole ring, earlywood, and latewood models, respectively (Fig. S1). A regression of observed versus predicted values of raw ring widths resulted in R^2 values of 0.84, 0.82, and 0.70, respectively (Fig. S1). Site-level R^2 ranged from 0.40 to 0.92 (Table S2), with the best model fits occurring for sites in the northern portion of the study area (sites 1, 2, 3, and 4, but also site 9; Table S2 and Fig. 1).

Parameter estimates

Based on the population of sites studied here, overall, tree growth was positively associated with precipitation (Fig. S2c), the precipitation × temperature interaction (Fig. S2e), and prior growth (Fig. S2f). Conversely, overall tree growth was negatively associated with age

(Fig. S2b) and earlywood growth (for the latewood model; Fig. S2g). Given the large variation in site-specific responses to temperature (Fig. 2d), the overall temperature effect tended towards negative, but was non-significant (Fig. S2d).

Focusing on the site-specific parameter estimates (e.g., Fig. 2), baseline annual growth ($a_{s,1,}$ back-transformed to mm) under average climate conditions varied by a factor of 2.4, ranging from 1.68 mm ± 0.08 (posterior mean ± SD; site 4, northern Arizona [AZ]) to 4.00 mm ± 0.22 (site 7, southern AZ) for the whole ring (Fig. 2a). Baseline earlywood growth was slightly less than whole-ring growth, and varied by a factor of 1.9 (range 1.53 mm ± 0.08 [site 4] to 2.91 mm ± 0.14 [site 8, southern New Mexico (NM)]), but baseline latewood growth was more consistent across sites with a mean of 0.37 mm (range 0.32 ± 0.03 [site 1, northern Utah (UT)] to 0.47 ± 0.03 [site 8]) (Fig. 2a). As expected, ring widths decreased with age for whole rings and earlywood ($a_{s,2} < 0$ in 9 sites in each model), but a smaller age effect was obvious in latewood widths ($a_{s,2} < 0$ for 5 sites and no significant relationship, $a_{s,2} \cong 0$, for 6 sites; Fig. 2b). Prior growth had a significant positive effect ($a_{s,6} > 0$) on ring width in all sites for all ring types (Fig. 2f). While earlywood and latewood widths were positively correlated with each other on initial study (Fig. S3), once the effects of climate, ring age, and prior ring width were accounted for, latewood width was significantly and negatively related to earlywood width ($a_{s,7} < 0$) of the same year in every site (Fig. 2g). Although sites were modeled hierarchically, which allows for sites with small sample sizes to be informed by other sites, those sites with fewer trees sampled were typically associated with more uncertain parameter estimates (wider CIs). This illustrates that the model is accounting for the unbalanced sample design.

Antecedent precipitation (P^{ant}) had a significant positive effect ($a_{t,3} > 0$) on whole-ring growth at eight sites and a significant negative effect ($a_{t,3} < 0$) in site 6, the most southern site

(Fig. 2c). Conversely, the direction of the antecedent temperature (T^{ant}) effects varied, with a significant positive effect ($a_{t,4} > 0$) occurring in three sites and a significant negative effect ($a_{t,4} < 0$) in six sites (Fig. 2d). While some sites were associated with non-significant P^{ant} (sites 4 and 5) or T^{ant} (sites 2 and 11) main effects, the $P^{ant} \times T^{ant}$ interaction effect ($a_{t,5}$) was significant across all sites (Fig. 2e), indicating that P^{ant} and T^{ant} are significant predictors of growth, either via their direct (main) effects and/or via their interaction with each other. In particular, the $P^{ant} \times T^{ant}$ interaction effect for whole rings was significantly different from zero for all sites; in all sites except one, the effect was positive, and in site 6 (southern AZ), it was negative. The generally positive $P^{ant} \times T^{ant}$ effect indicates that warmer conditions (higher T^{ant}) increase the (positive) sensitivity of growth to P^{ant}, or, alternatively, drier conditions (lower P^{ant}) enhance the negative effect of T^{ant} on growth. Effects of P^{ant}, T^{ant}, and $P^{ant} \times T^{ant}$ on earlywood growth were similar to the whole-ring effects in sign, magnitude, and significance, but they were generally of lower magnitude for latewood growth (Fig. 2c,d,e).

Antecedent importance weights

For most sites, the year of ring formation and the prior year had the highest annual precipitation weights for all three models (whole ring, earlywood, and latewood), indicating that growth is primarily governed by fairly recent precipitation inputs (Fig. S4). However, there were some exceptions; precipitation two years prior to growth was most important for whole-ring widths in sites 6 and 7 (southern AZ) (Fig. S4a) and for earlywood at those two sites as well as site 4 (northern AZ) (Fig. S4b). In site 5 (central AZ), precipitation received in all 5 years had nearly equal influence (weights) on whole ring and earlywood growth. Precipitation received in the year prior to growth was more important than the year of growth for predicting latewood width in 10 sites; only in site 2 (central Colorado [CO]) was the annual weight highest in the year

of growth (Fig. S4c). Temperature weights were also generally highest for the year of growth in all three models, with some exceptions (Fig. S4d,e,f). It is worth noting that if we had defined the annual period as October through September, annual weights would have been even higher for the current year.

Consistent with the annual importance weights, individual monthly weights were also generally highest in the year of and the year prior to ring formation, but variation in the monthly weights points to specific periods that are most important for predicting growth (Figs. S5a, S5b, S5c). In sites 1, 2, 3, and 4 (UT and northern AZ), which are among the coolest sites with the lowest annual precipitation, winter precipitation in the year of growth was important for whole ring (Fig. S5a) and earlywood growth (Fig. S5b), while in sites 5 and 6 (southern AZ), which are among the warmest sites, with most annual precipitation, winter precipitation two years prior to growth was more important than winter precipitation in the year of growth. For whole-ring and earlywood widths, temperature in the spring months during the year of ring formation was influential in most sites (Figs. S5a, S5b). For latewood widths (Fig. S5c), precipitation in the winter prior to ring formation was often as or more important than summer precipitation during the current growing season. Temperature during the spring and summer of the current growing season was influential in most sites.

At the sites with the highest precipitation and variability in precipitation (sites 5, 6, and 7 in southern AZ; Table S1), whole-ring widths had the longest climatic memory as measured by the M_{50} index for P^{ant} (Fig. 3a, Fig. S6a). Climatic memory of earlywood growth was similar to that of the whole-ring, although site 4 (northern AZ), which is characterized by moderate precipitation variability, had the longest M_{50} (31 months) for P^{ant} (Fig. 3b, Fig. S6b). There was less variation among sites in the latewood M_{50} values, which were generally unrelated to site-

318 level precipitation variability (Fig. 3c, Fig. S6c).

319 Sites with short climatic memory tended to have a positive, strong sensitivity to
320 precipitation, but a negative sensitivity to temperature (Fig. S7). With increasing M_{50} for P^{ant}, the
321 precipitation effects (P^{ant}; $a_{s,3}$) took on smaller, less positive values or even negative values.
322 However, with increasing M_{50} for T^{ant}, the T^{ant} effects ($a_{s,4}$) took on less negative values or even
323 positive values. In summary, the magnitudes of the P^{ant} and T^{ant} main effects, which are indices
324 of the climate sensitivities of growth, tended to be larger (more sensitive) for sites characterized
325 by shorter memory (lower M_{50}) (Fig. S7).

326 *Evaluation of site-level responses across climatic gradient*

327 Site-level sensitivity of growth to antecedent precipitation (i.e., as quantified by $a_{s,3}$;
328 Table 1) varied in relation to site-level climate characteristics (Fig. 4). Notably, the sensitivity of
329 whole-ring growth to antecedent precipitation at average temperature conditions, as described by
330 the site-level P^{ant} main effect ($a_{s,3}$), was not related to the proportion of precipitation falling in
331 the summer months (Table S3). However, the antecedent precipitation ($a_{s,3}$) effect for whole-ring
332 widths was negatively correlated with annual (Fig. 4a), winter (Fig. 4b), and summer (Fig. 4c)
333 precipitation totals (R^2 = 0.60, 0.69, and 0.27, respectively). The site-level earlywood and
334 latewood precipitation ($a_{s,3}$) effects were also negatively correlated with annual, summer, and
335 winter precipitation (earlywood R^2 = 0.48, 0.15, and 0.70, respectively; latewood R^2 = 0.72,
336 0.54, and 0.46, respectively).

337 Sites with higher annual and winter precipitation also had higher variability in annual and
338 winter precipitation (Fig. S8), and the antecedent precipitation (P^{ant}) main effect ($a_{s,3}$) was
339 strongly and negatively correlated with this variability (measured as standard deviation) in all
340 three ring type models. That is, the higher the standard deviation in annual and winter

341 precipitation, the less important antecedent precipitation was for growth (Table S3, Fig. 4d,e).
342 The precipitation effect ($a_{s,3}$) for latewood growth was negatively correlated with the standard
343 deviation of summer precipitation (Table S3, Fig. 4f). The antecedent temperature (T^{ant}) main
344 effect ($a_{s,4}$) and the $P^{ant} \times T^{ant}$ interaction effect ($a_{s,5}$) generally did not correlate with indices of
345 annual and seasonal precipitation amount or variation (Table S3), except for that the temperature
346 effect ($a_{s,4}$) for whole ring and earlywood growth was negatively correlated with summer
347 temperature ($p < 0.1$, Table S3).

348 **Discussion**

349 *Over what time scales are climate influences on tree growth evident?*

350 The trees in this study were sampled "ecologically" rather than for climate
351 reconstruction, which means they were not in particularly harsh conditions or near the edge of
352 their range (Nehrbass-Ahles et al. 2014), although they still occurred in semi-arid sites in the
353 southwestern US. Across all sites, the climate memory of tree growth was relatively long; while
354 climate conditions in the year of ring formation and one year prior were generally most
355 important for annual and sub-annual growth, climate conditions two, three, and four years prior
356 to ring formation were also influential. These results are consistent with other studies in the
357 Southwest that used International Tree-Ring Data Bank (ITRDB) records, from trees often
358 collected for climate reconstruction purposes, to examine relationships between tree growth and
359 climate at comparable time scales (Peltier et al. 2018). Using conifer tree-ring records from the
360 ITRDB in the Southwest, Peltier et al. (2018) employed the SAM approach and also found that
361 precipitation and temperature importance weights were highest in the year of growth (accounting
362 for nearly half the total weight) and the year prior to growth, but conditions 2-4 years prior to
363 growth still continued to influence growth. It is significant that we found similar evidence for

364 long climatic memory in trees using a different dataset collected for a different purpose,
365 suggesting that long climatic memory in trees is a widespread phenomenon not limited to highly
366 "sensitive" trees often chosen for paleo-climate reconstructions (Esper et al. 2015). We note
367 evidence for long memory of past climate in tree growth has been found worldwide, with
368 examples including *Pinus brutia* in the eastern Mediterranean, *P. pinea* in Italy, and multiple
369 species in the Spanish Pyrenees (Mazza and Manetti 2013, Marqués et al. 2021).

370 It is also worth pointing out that Szejner *et al*. (2020) found shorter legacies in carbon
371 isotope ratios and ring-width index in these same sites, using Superposed Epoch Analysis (SEA)
372 and detrended chronologies. There are several aspects that could explain these differences. First,
373 our analytical model focused on individual core and tree-level patterns rather than within-site
374 integration of individual chronologies, as used in Szejner *et al*. (2020). This difference likely
375 rendered our analysis more sensitive to the responses of individual tree phenotypes (i.e.,
376 endogenous factors), whereas the Szejner *et al*. (2020) analysis was more sensitive to site-to-site
377 and year-to-year climate variability (i.e., exogenous factors). Second, Szejner et al. (2020) found
378 that current year conditions were most important for tree growth, which our analysis also
379 generally shows (Fig. S4), but we also find that conditions during previous years are important.
380 In our study, the high importance of prior year's climate also captured the influence of the winter
381 months just preceding ring formation, which have been found to be important predictors of tree
382 growth in other studies (e.g., Martin et al. 2018). Finally, we did not focus on the most extreme
383 droughts as "key events" in this study, which is required in SEA. Rather, we analyzed the
384 influence of climate on tree growth across the entire period of the record, including all drought
385 events. It is possible that evidence of memory in drought sensitivity is most likely to be detected
386 when assessed across many droughts of variable intensity, rather than when focused on the most

387 extreme droughts. In analyses relying on the most extreme droughts, exogenous (climate-
388 determined) lags might be so dominant as to obscure endogenous (phenotype-determined) lags.
389 The latter might only emerge in analyses that include a broad range of climate system states
390 assessed across many years.

391 The long climatic memory reported here and elsewhere likely reflects an indirect effect of
392 past climate, mediated through various physical and physiological mechanisms. Possible
393 mechanisms for such lagged effects of climate on tree growth include retention of canopy
394 needles for several years, storage of non-structural carbohydrates (NSC) over multiple years,
395 hydraulic damage from prior drought, and pest or pathogen associations with drought-stressed
396 trees, among others (Peltier et al. 2018). *P. ponderosa* needles are usually retained for 3 to 4
397 years (Fritts 1976), meaning that an abundant or poor needle crop in a particular year could
398 positively or negatively impact growth for several years. The role of NSC in lagged growth
399 responses to climate is not fully understood. However, as average NSC pool ages can be nine or
400 more years old in conifer species in temperate forests (Richardson et al. 2012), and old NSC
401 (>15 yr) can be accessible (Carbone 2013), such old NSC could represent a functional link
402 between antecedent climate and current growth. Persistent hydraulic damage could also result in
403 long-lasting effects from water stress, particularly if functional sapwood area is significantly
404 reduced (Anderegg et al. 2015, Trugman et al. 2018, Peltier and Ogle 2019), or significant
405 changes in functional canopy area occur (Jump et al. 2017). Finally, pests and pathogens are
406 typically more successful in water-stressed trees (Jactel et al. 2012), providing another way that
407 climate variability, coupled with insect outbreaks, can have long lasting consequences for tree
408 vitality and growth (Peters et al. 2017). Physical effects may also be important; trees have access
409 to deep soil water resources, which integrate precipitation inputs over multiple seasons, but

410 which may also be depleted after severe drought events (Kerhoulas and Kane 2012, Rempe and
411 Dietrich 2018). Lagged effects of climate on tree growth are increasingly recognized as
412 important (e.g., Jiang et al. 2019), but focused experimental work is needed to understand the
413 mechanisms by which tree rings integrate climate over multiple years.

414 Varying climate responses at different sites across a precipitation gradient illustrate the
415 diversity of conditions experienced by *P. ponderosa* across the study region. A significant
416 growth versus antecedent precipitation relationship, which we expected, was observed in eight of
417 the 11 study sites (Fig. 2c). The lack of a direct effect of precipitation in two sites and a negative
418 effect in one site could be due to a precipitation x temperature interaction (see discussion below),
419 or unique precipitation distributions in the interannual sequence of the time series. These are
420 both examples of possible exogenous influences on climate memory effects. The direct effect of
421 temperature was more variable (Fig. 2d). Typically, temperature has a negative effect on tree
422 growth in the Southwest because of its link to increased drought stress (Williams et al. 2013,
423 Adams and Kolb 2005), which appears to occur in six sites. However, warmer temperatures were
424 positively correlated with tree growth in two sites (sites 7 and 8), both of which are in the
425 southern portion of the study area (Fig. 1) and are associated with comparatively high rainfall
426 (Table S1) and high baseline growth (Fig. 2a). This suggests that when trees have access to
427 greater soil moisture, higher antecedent temperatures lead to greater productivity, potentially due
428 to the effect of warm, but not extreme, temperatures on physiological processes involved in
429 carbon gain, allocation, and biomass production (Way and Oren 2010).

430 It is not surprising that antecedent temperature and precipitation interact to govern tree
431 growth across the precipitation gradient in the Southwest. However, the net effect of this
432 interaction indicates the existence of a synergistic impact leading to increased sensitivity of tree

433 growth to the combination of hotter and drier conditions, or what might be referred to as hot
434 drought (Overpeck 2013). This has been documented on a temporal scale where drier sites
435 showed increasing growth sensitivity to PDSI over the last century, paralleled by higher
436 mortality following the ongoing drought in California (Keen et al. 2021). Similar changes in
437 growth sensitivity to climate have been reported across precipitation gradients in different
438 functional types (Kannenberg et al. 2022) and between different biomes (Hsu et al. 2012,
439 Gherardi and Sala 2019, Maurer et al. 2020, O'Donnell et al. 2021). We would expect these
440 trends to continue given projections of rising temperatures (Zobel et al. 2017).
441 *Do tree growth sensitivity to climate and ecological memory vary across the precipitation*
442 *gradient?*
443 Relationships between tree growth and climate did vary across the precipitation gradient,
444 but percent summer (monsoon) precipitation provided little insight into spatial variation in
445 climate-growth relationships. We suggest that the NAM gradient is only one gradient among
446 several in this complex region that governs tree and forest productivity (Gutzler 2004). We did
447 find that the total amount of precipitation and associated monthly variation were important in
448 influencing tree growth. Sites 5, 6, and 7 in central and southern Arizona (AZ) stood out in
449 several analyses: they had the highest standard deviations in monthly precipitation (Table S1),
450 they are 3 of the 4 wettest sites (Table S1), and they had 3 of the 4 lowest precipitation main
451 effect sizes (Fig. 2c). The finding that these wet sites supported *P. ponderosa* trees with lower
452 precipitation sensitivity, under average temperature conditions, is consistent with past studies
453 and was expected. For example, Adams and Kolb (2005) found that tree growth of several
454 conifer species in higher, wetter sites in AZ was less sensitive to drought than in lower, drier
455 sites. The lower precipitation sensitivity of tree growth under average temperature conditions in

these sites suggests that trees are following a conservative strategy, in which they are not capable of physiological plasticity that would permit increased or decreased growth to track shifting conditions. It is also possible that in these wetter sites something besides moisture (e.g. nutrient limitations or cloud cover) is limiting tree growth during wet periods such that additional precipitation does not result in high growth in very wet years (Chapin et al. 1987). Trees in drier sites are generally more sensitive to precipitation, indicating that they may be most affected by changes to the total amount or timing of precipitation (Anderegg et al. 2019).

In our study, lower climate sensitivity was associated with longer climatic memory (Fig. S7). This combination of low effect size and long memory implies a muted response to climate; trees in these variable sites are not responsive to every pulse of rain but integrate climate (e.g., precipitation pulses) over many seasons and years. In these sites, if a tree allocates additional carbon resources to roots, canopy expansion, or wider than average rings in a wet year, the wet year could have a long-lasting influence on tree growth. Alternately, when a dry year occurs, a poor needle crop (Fritts 1976) or a loss of roots (Brunner et al. 2015) may necessitate a longer recovery time; effects may be long-lasting even if subsequent years have abundant rainfall (e.g., Anderegg et al. 2015). Trees that receive less summer precipitation might have the ability to "immediately" take advantage of rain events, making their growth more sensitive to recent conditions (shorter memory, lower M_{50}). We might hypothesize that trees at these sites would have faster carbon cycling rates and younger NSC. The finding that higher climatic sensitivity is associated with shorter climatic memory is interesting in the context of the ongoing discussions about biases in the ITRDB (Klesse et al. 2018). First, any bias in ITRDB is likely in the magnitude of the climate-growth responses, and not in the direction or character of the relationships. In addition, short climatic memory of sensitive trees is a positive attribute for

climate or disturbance reconstructions, since multi-year memory in tree rings can bias or contaminate climatic or disturbance signals (Esper et al. 2015, Esper et al. 2018).

Do earlywood and latewood growth differ in their sensitivities to climate and climatic memory?

For both climatic sensitivity and memory, site differences were readily apparent in earlywood growth attributes. However, latewood growth was fairly invariant across sites in terms of baseline growth under average conditions. This may be due to little variation in the onset of latewood formation in *P. ponderosa*, even in years with very different precipitation patterns (Ziaco et al. 2018). However, the finding of greater variability in earlywood widths may be species-specific; in some species, latewood widths vary more than earlywood widths, but in other species the opposite occurs (e.g., Miina 2000). Climatic memory was quite different between earlywood and latewood as well (Fig. S6); latewood memory was shorter and less variable between sites, but climate in years prior to growth was still important.

While climate influenced latewood growth, the strongest factor associated with low latewood growth was simply high earlywood growth (negative effect across all 11 sites). This should not be confused with positive correlations between raw earlywood and latewood widths, which are observed in simple bivariate plots or correlation analyses (Fig. S3, Meko and Baisan 2001, Griffin et al. 2011). Instead, this earlywood effect should be thought of as the conditional effect of earlywood growth given that climate, ring age, and past ring width effects are accounted for. This suggests that after accounting for the effects of climate, age, and past widths, which tend to have the same directional effects on earlywood and latewood growth, the conditional effect of earlywood on latewood growth is actually negative, pointing to a tradeoff between these two modes of radial growth. This tradeoff could be related to carbon resources; if a tree invests a great deal of carbon in earlywood (or earlywood formation runs longer), there may be less

carbon (or time) to invest in latewood growth. This idea is supported by isotopic analysis of the same trees used in this study; isotope signals in earlywood and latewood were generally positively correlated (Szejner et al. 2018), suggesting that trees use the same resources to produce earlywood and latewood. Alternatively, the tradeoff could be related to xylogenesis and phenology mechanisms (Ziaco et al. 2018). It is thought that earlywood is important for water transport and latewood is important for tree structure; each year's growth represents a balance between a tree's maintenance of these two functions of xylem (Björklund et al. 2017). Future research might explore whether allocation between these competing functions may be altered by recent climate conditions, particularly drought. For example, an adaptive strategy would be to invest relatively more carbon towards earlywood growth following severe cavitation events to efficiently regain pre-drought sapwood area (Trugman et al. 2018). Finally, the possibility of a carbon allocation tradeoff between earlywood and latewood has implications for climate reconstructions when using any type of tree ring data: whole ring, earlywood, or latewood.

Conclusions

Our study of *Pinus ponderosa* in the Southwest showed that tree growth responses to climate and the timescales over which growth responds to climate varied across the regional precipitation gradient. Severe summer drought has been observed over the period 2000-2018 (Williams et al. 2020) due to anthropogenic warming, and the North American Monsoon may experience changes such as a delayed onset and shifts in precipitation distribution to later in the season (Cook and Seager 2013). Our results suggest that such future changes to precipitation patterns will have unequal effects on tree growth across the regional precipitation gradient, with potential implications for tree growth and mortality, carbon storage, and regional species migrations.

Acknowledgements

We thank the Ogle lab group for feedback on earlier versions of this manuscript.

Declarations

Funding: The majority of the work conducted in this study was funded by a National Science Foundation-Advances in Biological Informatics grant to K. Ogle (#1458867). P. Szejner and R. Monson acknowledge financial support from the Macrosystems Program in the Emerging Frontiers Section of the U.S. National Science Foundation (#1065790) and the Ecosystems Program in the Division of Environmental Biology (#1754430), which enabled much of the sampling and data collection. Y. Liu was partly supported by the U.S. Department of Energy contract DE-AC05-00OR22725.

Conflicts of Interest: The authors declare that they have no conflict of interest.

Ethics approval: Ethics approval was not required for this study.

Consent to participate: Not applicable.

Consent for publication: Not applicable.

Availability of data and material: All data for this manuscript will be posted in the International Tree-Ring Database (ITRDB).

Code availability: Code is available from corresponding author upon request.

Author contributions: LLY and KO conceived of the idea. PS and RKM collected the data. LLY, KO and DP analyzed the data. LLY wrote the manuscript; all authors provided editorial advice.

548 **References**

549 Adams DK, Comrie AC (1997) The North American monsoon. Bull Am Meteorol Soc 78:2197–
550 2214. https://doi.org/10.1175/1520-0477(1997)078<2197:TNAM>2.0.CO;2
551 Adams DK, Minjarez C, Serra Y, Quintanar A, Alatore L, Granados A, Vásquez E, Braun J
552 (2014) Mexican GPS tracks convection from North American Monsoon. Eos, Trans Am
553 Geophys Union 95:61–62. https://doi.org/10.1002/2014EO070001
554 Adams, HD, Kolb TE (2005) Tree growth response to drought and temperature in a mountain
555 landscape in northern Arizona, USA. J Biogeogr 32:1629–1640.
556 https://doi.org/10.1111/j.1365-2699.2005.01292.x
557 Anderegg WRL, Schwalm C, Biondi F, Camarero JJ, Koch G, Litvak M, Ogle K, Shaw JD,
558 Shevliakova E, Williams AP, Wolf A, Ziaco E, Pacala S (2015) Pervasive drought legacies in
559 forest ecosystems and their implications for carbon cycle models. Science 349:528–532.
560 https://doi.org/10.1126/science.aab1833
561 Anderegg WRL, Anderegg LDL, Kerr KL, Trugman AT (2019) Widespread drought-induced
562 tree mortality at dry range edges indicates climate stress exceeds species' compensating
563 mechanisms. Glob Change Biol 25:3793-3802. https://doi.org/10.1111/gcb.14771
564 Babst F, Wright WE, Szejner P, Wells L, Belmecheri S, Monson RK (2016) Blue intensity
565 parameters derived from Ponderosa pine tree rings characterize intra-annual density
566 fluctuations and reveal seasonally divergent water limitations. Trees 30:1403–1415.
567 https://doi.org/10.1007/s00468-016-1377-6
568 Belmecheri S, Wright WE, Szejner P, Morino KA, Monson RK (2018) Carbon and oxygen
569 isotope fractionations in tree rings reveal interactions between cambial phenology and seasonal
570 climate. Plant Cell Environ 41:2758–2772. https://doi.org/10.1111/pce.13401

Björklund J, Seftigen K, Schweingruber F, Fonti P, von Arx G, Bryukhanova MV, Cuny HE, Carrer M, Castagneri D, Frank DC (2017) Cell size and wall dimensions drive distinct variability of earlywood and latewood density in Northern Hemisphere conifers. New Phytol 216:728–740. https://doi.org/10.1111/nph.14639

Brunner I, Herzog C, Dawes MA, Arend M, Sperisen C (2015) How tree roots respond to drought. Front Plant Sci 6:547. https://doi.org/10.3389/fpls.2015.00547

Chapin FS, Bloom AJ, Field CB, Waring RH (1987) Plant responses to multiple environmental factors. BioScience 37: 49-57. https://doi.org/1310177

Cook BI, Seager R (2013) The response of the North American Monsoon to increased greenhouse gas forcing. JGR Atmospheres 118:1690–1699. https://doi.org/10.1002/jgrd.50111

Douglas MW, Maddox RA, Howard K, Reyes S (1993) The Mexican Monsoon. J Climate 6:1665–1677. https://doi.org/10.1175/1520-0442(1993)006<1665:TMM>2.0.CO;2

Esper JL, Schneider L, Smerdon JE, Schöne BR, Büntgen U (2015) Signals and memory in tree-ring width and density data. Dendrochronologia 35:62-70. https://doi.org/10.1016/j.dendro.2015.07.001

Esper J, St. George S, Anchukaitis K, D'Arrigo R, Ljungqvist FC, Luterbacher J, Schneider L, Stoffel M, Wilson R, Büntgen U (2018) Large-scale, millennial-length temperature reconstructions from tree-rings. Dendrochronologia 50:81-90. https://doi.org/10.1016/j.dendro.2018.06.001

Fritts HC (1976) Tree rings and climate. Academic Press, London ; New York.

Gherardi LA, Sala OE (2019) Effect of interannual precipitation variability on dryland productivity: A global synthesis. Glob Chang Biol 25:269-76. https://doi.org/10.1111/gcb.14480

Griffin D, Meko DM, Touchan R, Leavitt SW, Woodhouse CA (2011) Latewood chronology development for summer-moisture reconstruction in the US Southwest. Tree-Ring Res 67:87–101. https://doi.org/10.3959/2011-4.1

Griffin D, Woodhouse CA, Meko DM, Stahle DW, Faulstich HL, Carrillo C, Touchan R, Castro CL, Leavitt SW (2013) North American monsoon precipitation reconstructed from tree-ring latewood. Geophys Res Lett 40:954–958. https://doi.org/10.1002/grl.50184

Guo JS, Hultine KR, Koch GW, Kropp H, Ogle K (2020) Temporal shifts in iso/anisohydry revealed from daily observations of plant water potential in a dominant desert shrub. New Phytol 225:713-726. https://doi.org/10.1111/nph.16196

Gutzler DS (2004) An index of interannual precipitation variability in the core of the North American Monsoon region. J Climate 17:4473-4480. https://doi.org/10.1175/3226.1

Higgins RW, Yao Y, Wang XL (1997) Influence of the North American Monsoon System on the U.S. summer precipitation regime. J Climate 10:2600–2622. https://doi.org/10.1175/1520-0442(1997)010<2600:IOTNAM>2.0.CO;2

Higgins RW, Chen Y, Douglas AV (1999) Interannual variability of the North American warm season precipitation regime. J Climate 12:653–680. https://doi.org/10.1175/1520-0442(1999)012<0653:IVOTNA>2.0.CO;2

Higgins RW, Douglas A, Hahmann A, Berbery EH, Gutzler D, Shuttleworth J, Stensrud D, Amador J, Carbone R, Cortez M, Douglas M, Lobato R, Meitin J, Ropelewski C, Schemm J, Schubert S, Zhang C (2003) Progress in Pan American CLIVAR Research: The North American Monsoon System. Atmósfera 16:29–65.

Hsu JS, Powell J, Adler PB (2012) Sensitivity of mean annual primary production to precipitation. Glob Change Biol 18:2246–55. https://doi.org/10.1111/j.1365-

2486.2012.02687.x

Jactel H, Petit J, Desprez-Loustau ML, Delzon S, Piou D, Battisti A, Koricheva J (2012) Drought effects on damage by forest insects and pathogens: a meta-analysis. Glob Change Biol 18:267–276. https://doi.org/10.1111/j.1365-2486.2011.02512.x

Jiang P, Liu H, Piao S, Ciais P, Wu X, Yin Y, Wang H (2019) Enhanced growth after extreme wetness compensates for post-drought carbon loss in dry forests. Nat Comm 10:195. https://doi.org/10.1038/s41467-018-08229-z

Jump AS, Ruiz-Benito P, Greenwood S, Allen CD, Kitzberger T, Fensham R, Martínez-Vilalta J, Lloret F (2017) Structural overshoot of tree growth with climate variability and the global spectrum of drought-induced forest dieback. Glob Change Biol 23:3742–3757. https://doi.org/10.1111/gcb.13636

Kannenberg SA, Driscoll A , Szejner P, Anderegg W, Ehleringer J (2021) Rapid increases in shrubland and forest intrinsic water-use efficiency during an ongoing megadrought. PNAS 118(52): e2118052118. https://doi.org/10.1073/pnas.2118052118

Keen RM, Voelker SL, Wang SYS, Bentz BJ, Goulden M, Dangerfield CR, Reed CC, Hood SM, Csank AZ, Dawson TE, Merschel AG, Still CJ (2022) Changes in tree drought sensitivity provided early warning signals to the California drought and forest mortality event. Glob Change Biol 28:1119-1132. https://doi.org/10.1111/gcb.15973

Kerhoulas LP, Kane JM (2012) Sensitivity of ring growth and carbon allocation to climatic variation vary within ponderosa pine trees. Tree Physiol 32:14–23. https://doi.org/10.1093/treephys/tpr112

Klesse S, DeRose RJ, Guiterman CH, Lynch AM, O'Connor CD, Shaw JD, Evans MEK (2018) Sampling bias overestimates climate change impacts on forest growth in the SW United States.

Nature Comm. 9:5336. Sampling bias overestimates climate change impacts on forest growth in the SW United States

Liu Y, Schwalm CR, Samuels-Crow KE, Ogle K (2019) Ecological memory of daily carbon exchange across the globe and its importance in drylands. Ecol Lett 22:1806-1816. https://doi.org/10.1111/ele.13363

Marqués L, Peltier DMP, Camarero J., Zavala MA, Madrigal-González J, Sangüesa-Barreda G, Ogle K (2021) Disentangling the legacies of climate and management on tree growth. Ecosystems 1-21. https://doi.org/10.1007/s10021-021-00650-8

Martin J, Looker N, Hoylman Z, Jencso K, Hu J (2018) Differential use of winter precipitation by upper and lower elevation Douglas fir in the Northern Rockies. Glob Change Biol 24: 5607-5621. https://doi.org/10.1111/gcb.14435

Maurer GE, Hallmark AJ, Brown RF, Sala OE, Collins SL (2020) Sensitivity of primary production to precipitation across the United States. Ecol Lett 23:527–36. https://doi.org/10.1111/ele.13455

Mazza G, Manetti MC (2013) Growth rate and climate responses of *Pinus pinea* L. in Italian coastal stands over the last century. Climatic Change 121:713–725. https://doi.org/10.1007/s10584-013-0933-y

McDowell NG, Allen CD, Marshall L (2010) Growth, carbon-isotope discrimination, and drought-associated mortality across a *Pinus ponderosa* elevational transect. Glob Change Biol 16:399-415. https://doi.org/10.1111/j.1365-2486.2009.01994.x

Meko DM, Baisan CH (2001) Pilot study of latewood-width of conifers as an indicator of variability of summer rainfall in the North American monsoon region. Int J Climatol 21: 697–708. https://doi.org/10.1002/joc.646

663 Miina J (2000) Dependence of tree-ring, earlywood and latewood indices of Scots pine and
664 Norway spruce on climatic factors in eastern Finland. Ecol Model 132:259–273.
665 https://doi.org/10.1016/S0304-3800(00)00296-9
666 Monson RK, Szejner P, Belmecheri S, Morino K, Wright WE (2018) Finding the seasons in tree
667 ring stable isotopes. Am J Bot 105:819–821. http://doi.org/10.1002/ajb2.1083
668 Nehrbass-Ahles C, Babst F, Klesse S, Nötzli M, Bouriaud O, Neukom R, Dobbertin M, Frank D
669 (2014) The influence of sampling design on tree-ring-based quantification of forest growth.
670 Glob Change Biol 20:2867-2885. https://doi.org/10.1111/gcb.12599
671 Neilson RP (1987) Biotic regionalization and climatic controls in western North America.
672 Vegetatio 70:135–147. https://doi.org/10.1007/BF00039327
673 O'Donnell AJ, Renton M, Allen KJ, Grierson PF (2021) Tree growth responses to temporal
674 variation in rainfall differ across a continental-scale climatic gradient. Plos One 16:e0249959.
675 https://doi.org/10.1371/journal.pone.0249959
676 Ogle K, Barber JJ, Barron-Gafford GA, Bentley LP, Young JM, Huxman TE, Loik ME, Tissue
677 DT (2015) Quantifying ecological memory in plant and ecosystem processes. Ecol Lett
678 18:221–235. https://doi.org/10.1111/ele.12399
679 Overpeck JT (2013) Climate science: The challenge of hot drought. Nature 503:350–351.
680 https://doi.org/10.1038/503350a
681 Peltier DMP, Ogle K (2019) Legacies of La Niña: North American monsoon can rescue trees
682 from winter drought. Glob Change Biol 25:121-133. https://doi.org/10.1111/gcb.14487
683 Peltier DMP, Fell M, Ogle K (2016) Legacy effects of drought in the southwestern United
684 States: A multi-species synthesis. Ecol Monogr 86:312–326. https://doi.org/10.1002/ecm.1219
685 Peltier DMP, Barber JJ, Ogle K (2018) Quantifying antecedent climatic drivers of tree growth in

the Southwestern US. J Ecol 106:613–624. https://doi.org/10.1111/1365-2745.12878

Peltier DMP, Guo J, Nguyen P, Bangs M, Gear L, Wilson M, Jefferys S, Samuels-Crow K, Yocom LL, Liu Y, Fell MK, Auty D, Schwalm C, Anderegg WRL, Koch GW, Litvak ME, Ogle K (2022) Temperature memory and non-structural carbohydrates mediate legacies of a hot drought in trees across the southwestern USA. Tree Physiol 42:71-85. https://doi.org/10.1093/treephys/tpab091

Peters RL, Klesse S, Fonti P, Frank DC (2017) Contribution of climate vs. larch budmoth outbreaks in regulating biomass accumulation in high-elevation forests. Forest Ecol Manag 401:147–158. https://doi.org/10.1016/j.foreco.2017.06.032

Plummer M (2003) JAGS: A program for analysis of Bayesian graphical models using Gibbs sampling. 3rd international workshop on distributed statistical computing. Vienna.

Plummer M (2013) rjags-package: Bayesian graphical models using MCMC in rjags: Bayesian Graphical Models using MCMC.

Plummer M, Best N, Cowles K, Vines K (2006) CODA: convergence diagnosis and output analysis for MCMC. R News 6:7–11.

PRISM Climate Group (2018) Climate data. http://prism.oregonstate.edu/.

R Core Team (2021) R: A Language and Environment for Statistical Computing. R Foundation for Statistical Computing.

Rempe DM, Dietrich WE (2018) Direct observations of rock moisture, a hidden component of the hydrologic cycle. P Natl Acad Sci USA 115:2664–2669. https://doi.org/10.1073/pnas.1800141115

Richardson AD, Carbone MS, Keenan TF, Czimczik CI, Hollinger DY, Murakami P, Schaberg PG, Xu X (2012) Seasonal dynamics and age of stemwood NSCs in temperate forests. New

709 Phytol 197:850–861. https://www.jstor.org/stable/newphytologist.197.3.850
710 Salzer MW, Kipfmueller KF (2005) Reconstructed temperature and precipitation on a millennial
711 timescale from tree-rings in the southern Colorado Plateau, U.S.A. Climatic Change 70:465–
712 487. https://doi.org/10.1007/s10584-005-5922-3
713 Stahle DW, Cleaveland MK, Grissino-Mayer HD, Griffin RD, Fye FK, Therrell MD, Burnette
714 DJ, Meko DM, Villanueva Diaz J (2009) Cool- and warm-season precipitation reconstructions
715 over western New Mexico. J Climate 22:3729–3750. https://doi.org/10.1175/2008JCLI2752.1
716 Stokes MA, Smiley TL (1968) An introduction to tree-ring dating. University of Chicago Press,
717 Chicago, Illinois.
718 Szejner P, Wright WE, Babst F, Belmecheri S, Trouet V, Leavitt SW, Ehleringer JR, Monson
719 RK (2016) Latitudinal gradients in tree ring stable carbon and oxygen isotopes reveal
720 differential climate influences of the North American Monsoon System. J Geophy Res Biogeo
721 121:1978–1991. https://doi.org/10.1002/2016JG003460
722 Szejner P, Wright WE, Belmecheri S, Meko D, Leavitt SW, Ehleringer JR, Monson RK (2018)
723 Disentangling seasonal and interannual legacies from inferred patterns of forest water and
724 carbon cycling using tree-ring stable isotopes. Glob Change Biol 24:5332–5347.
725 https://doi.org/10.1111/gcb.14395
726 Szejner P, Belmecheri S, Ehleringer JR, Monson RK (2020) Recent increases in drought
727 frequency cause observed multi-year drought legacies in the tree rings of semi-arid forests.
728 Oecologia 192:241-259. https://doi.org/10.1007/s00442-019-04550-6
729 Szejner P, Belmecheri S, Babst F, Wright WE, Frank DC, Hu J, Monson RK (2021) Stable
730 isotopes of tree rings reveal seasonal-to-decadal patterns during the emergence of a
731 megadrought in the Southwestern U.S. Oecologia 197:1079-1094.

https://doi.org/10.1007/s00442-021-04916-9

Trugman AT, Detto M, Bartlett MK, Medvigy D, Anderegg WRL, Schwalm C, Schaffer B, Pacala SW (2018) Tree carbon allocation explains forest drought-kill and recovery patterns. Ecol Lett 21:1552-1560. https://doi.org/10.1111/ele.13136

Way DA, Oren R (2010) Differential responses to changes in growth temperature in trees from different functional groups and biomes: a review and synthesis of data. Tree Physiol 30: 669-688. https://doi.org/10.1093/treephys/tpq015

Williams AP, Allen CD, Macalady AK, Griffin D, Woodhouse CA, Meko DM, Swetnam TW, Rauscher SA, Seager R, Grissino-Mayer HD, Dean JS, Cook ER, Gangodagamage C, Cai M, McDowell NG (2013) Temperature as a potent driver of regional forest drought stress and tree mortality. Nat Clim Change 3:292–297. https://doi.org/10.1038/nclimate1693

Williams AP, Cook ER, Smerdon JE, Cook BI, Abatzoglou JT, Bolles K, Baek SH, Badger AM, Livneh B (2020) Large contribution from anthropogenic warming to an emerging North American megadrought. Science 368:314-318. https://doi.org/10.1126/science.aaz9600

Zhang W, Shi J, Y. Zhao, Shi S, Ma X, Zhu Y (2021) December-March temperature reconstruction from tree-ring earlywood width in southeastern China during the period of 1871-2016. Int J Biometeorol 65:883-894. https://doi.org/10.1007/s00484-020-02067-9

Ziaco E, Truettner C, Biondi F, Bullock S (2018) Moisture-driven xylogenesis in *Pinus ponderosa* from a Mojave Desert mountain reveals high phenological plasticity. Plant Cell Environ 41:823–836. https://doi.org/10.1111/pce.13152

Zobel Z, Wang J, Wuebbles J, Rao Kotamarthi V (2017) High-resolution dynamical downscaling ensemble projections of future extreme temperature distributions for the United States. Earth's Future 5:1234–1251. https://doi.org/10.1002/2017EF000642

Figure Legends

Figure 1. Eleven sites where *Pinus ponderosa* trees were sampled in the southwestern USA (UT: Utah, AZ: Arizona, NM: New Mexico, CO: Colorado). Color gradient represents a) % precipitation that falls in summer (July, August, and September), b) mean total annual precipitation, and c) standard deviation of precipitation. See Table S1 for details on each site.

Figure 2. Posterior means (symbols) and 95% Bayesian credible intervals (whiskers) for study-level parameters, including a) baseline growth (intercept; $a_{s,1}$) and the effects of b) age (A; $a_{s,2}$), c) antecedent precipitation (P^{ant}; $a_{s,3}$), d) antecedent temperature (T^{ant}; $a_{s,4}$), e) the $P^{ant} \times T^{ant}$ interaction ($a_{s,5}$), f) prior ring-width ($a_{s,6}$), and g) earlywood width for latewood ($a_{s,7}$); see Eqn (2) and Table 1. Parameters with CIs not crossing zero are interpreted as reflecting important ("significant") effects. Sites are ordered by mean annual precipitation (low to high).

Figure 3. Linear regressions between site-level precipitation memory (M_{50}; the month prior to December of the current year at which the cumulative weights first exceed 0.5) and a) winter precipitation, b) summer precipitation, c) elevation, d) yearly precipitation standard deviation (SD), e) winter precipitation SD, f) summer precipitation SD, g) annual temperature, and h) winter temperature. Only significant relationships are shown: symbols indicate $p < 0.01$, and regression lines indicate $p < 0.05$ (Table S4). Black circles/lines represent whole-ring widths (RW), white squares/dashed lines represent earlywood (EW), and gray triangles/lines represent latewood (LW).

Figure 4. Linear regressions between site-level antecedent precipitation (P^{ant}) main effects ($a_{s,3}$) and a) annual, b) winter, c) summer precipitation, d) annual, e) winter, and f) summer precipitation stand deviation. All relationships with regression lines are significant ($p < 0.05$; Table S3). Black circles/lines represent whole-ring widths, white squares/dashed lines represent

778 earlywood, and gray triangles/lines represent latewood. Blue lines cross the y-axis at 0. Whiskers
779 depict 95% Bayesian credible intervals.

Tables

Table 1. Summary of coefficients in the stochastic antecedent modeling (SAM) regression model (Eqn 2). The subscripts t and s denote tree t and site s.

Symbol		Definition
Tree-level	Site-level	
$\alpha_{t,1}$	$a_{s,1}$	Intercept; predicted growth at average age and climate
$\alpha_{t,2}$	$a_{s,2}$	Age effect
$\alpha_{t,3}$	$a_{s,3}$	Antecedent precipitation effect
$\alpha_{t,4}$	$a_{s,4}$	Antecedent temperature effect
$\alpha_{t,5}$	$a_{s,5}$	Antecedent precipitation × antecedent temperature effect
$\alpha_{t,6}$	$a_{s,6}$	Prior ring width effect
$\alpha_{t,7}$	$a_{s,7}$	Effect of earlywood on latewood growth (only in latewood model)

Fig. 1

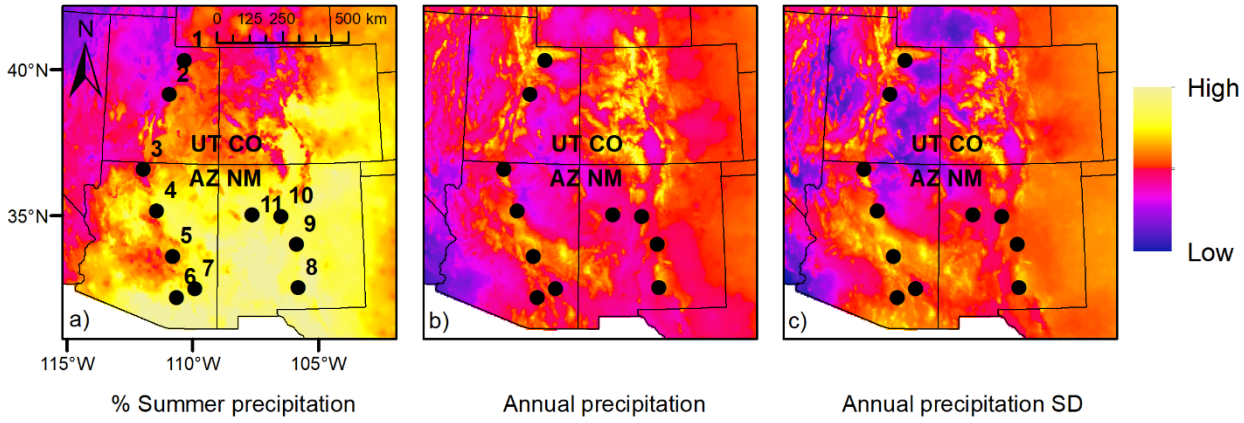
N
0 125 250 500 km
40°N
35°N
115°W
110°W
105°W
1
2
3
4
5
6
7
8
9
10
11
UT CO
AZ NM
a)
b)
c)
High
Low
% Summer precipitation
Annual precipitation
Annual precipitation SD

Fig. 2

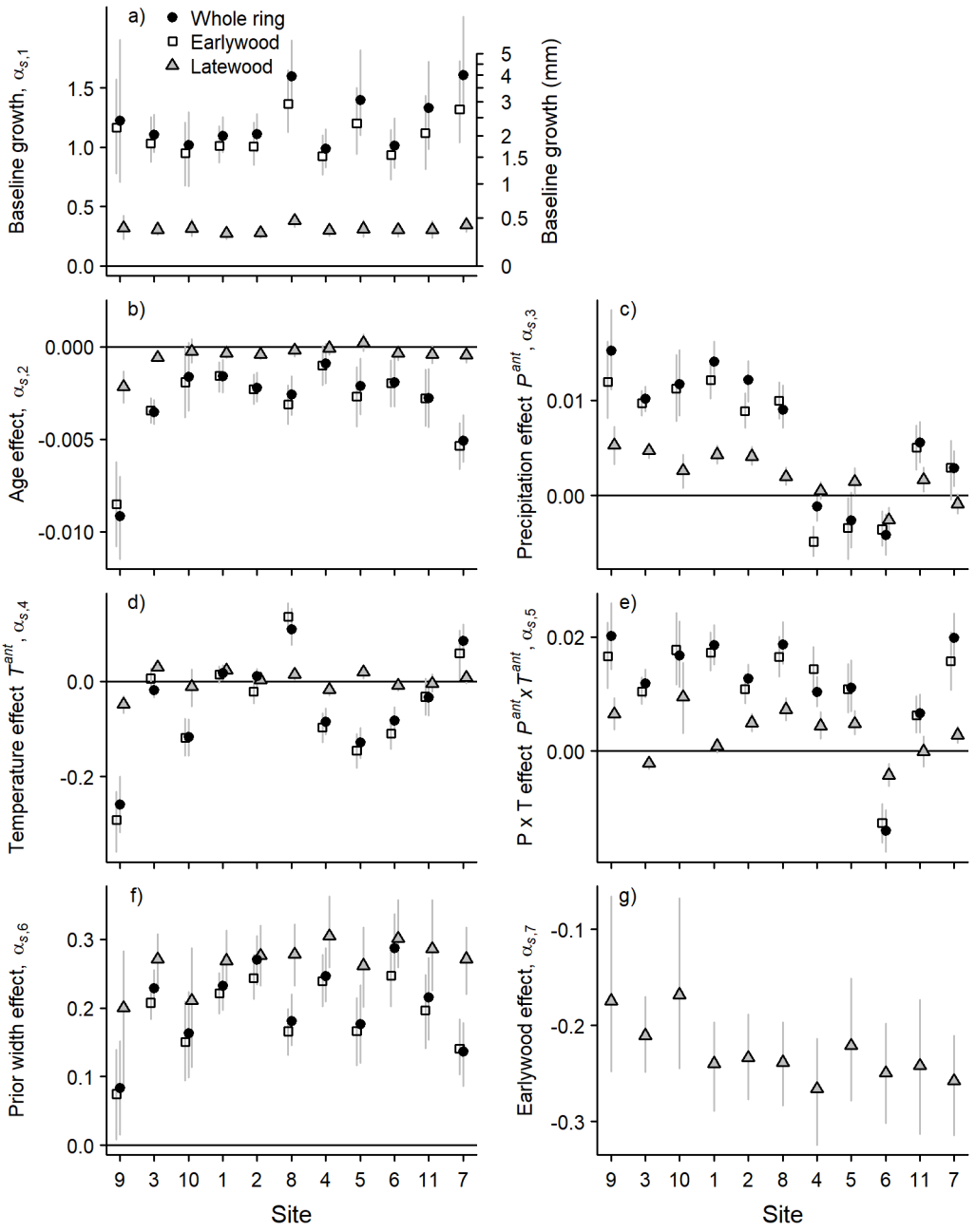
a)
Whole ring
Earlywood
Latewood
Baseline growth, $\alpha_{s,1}$
Baseline growth (mm)
b)
Age effect, $\alpha_{s,2}$
c)
Precipitation effect P^{ant}, $\alpha_{s,3}$
d)
Temperature effect T^{ant}, $\alpha_{s,4}$
e)
P x T effect P^{ant}x T^{ant}, $\alpha_{s,5}$
f)
Prior width effect, $\alpha_{s,6}$
g)
Earlywood effect, $\alpha_{s,7}$
9 3 10 1 2 8 4 5 6 11 7
Site

Fig. 3

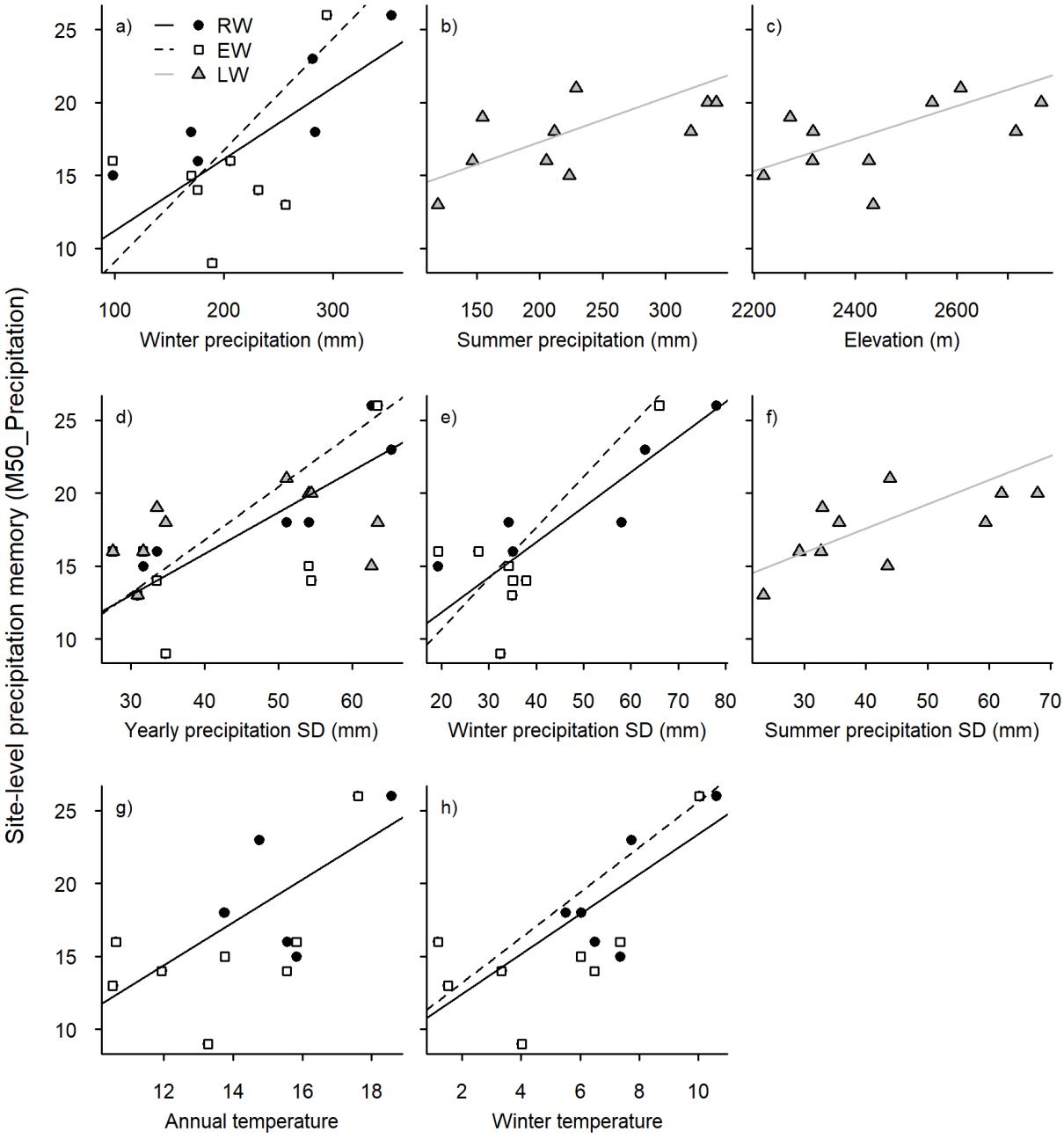
a)
RW
EW
LW
b)
c)
d)
e)
f)
g)
h)
Site-level precipitation memory (M50_Precipitation)
Winter precipitation (mm)
Summer precipitation (mm)
Elevation (m)
Yearly precipitation SD (mm)
Winter precipitation SD (mm)
Summer precipitation SD (mm)
Annual temperature
Winter temperature

Fig. 4

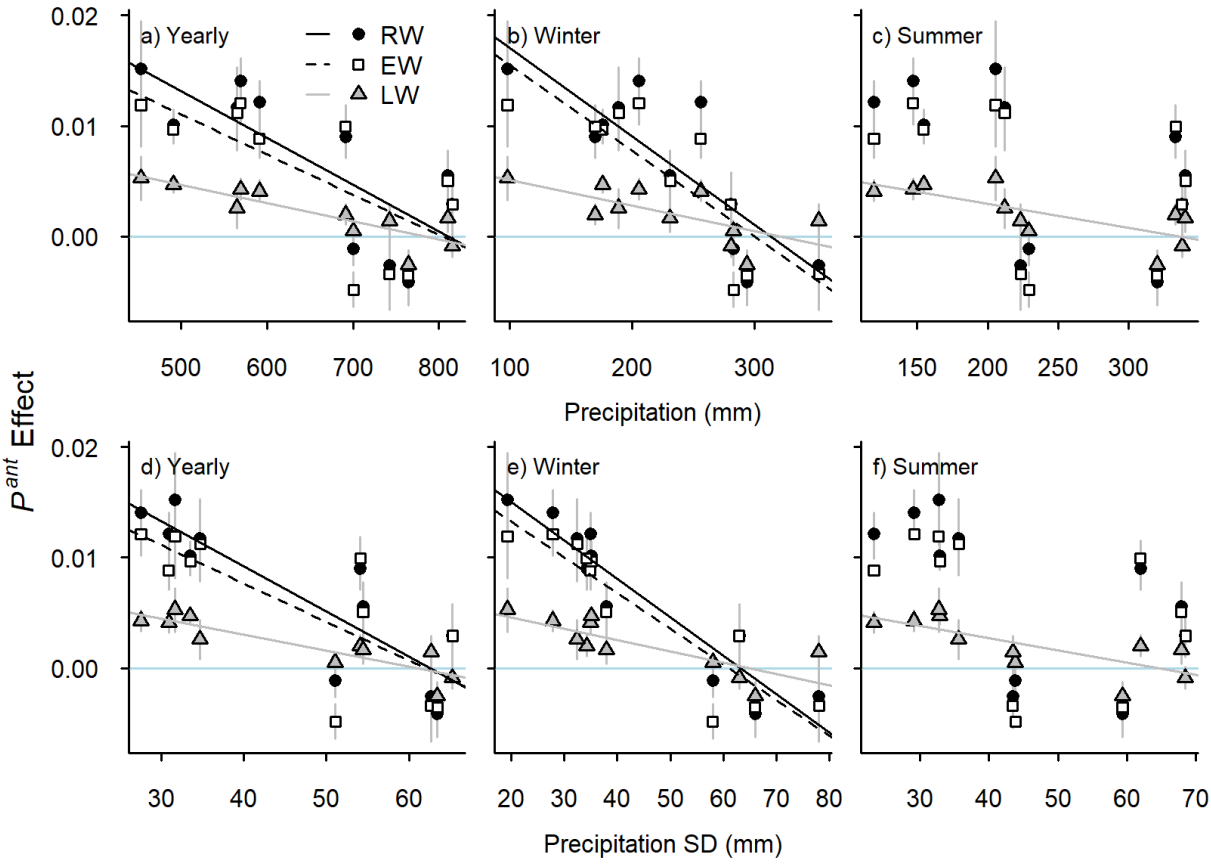
a) Yearly
b) Winter
c) Summer
d) Yearly
e) Winter
f) Summer
RW
EW
LW
P^{ant} Effect
0.02
0.01
0.00
500
600
700
800
100
200
300
150
200
250
300
Precipitation (mm)
30
40
50
60
20
70
80
Precipitation SD (mm)